# Artificial Neural Network Aided Cable Resistance Estimation in Droop-Controlled Islanded DC Microgrids

Habibu Hussaini [1,2*], Tao Yang [1], Yuan Gao [1], Cheng Wang [1], Mohamed A. A. Mohamed[1], Serhiy Bozhko [1]
[1] Power Electronics, Machines and Control (PEMC) Research Group, Faculty of Engineering, University of Nottingham, Nottingham, NG7 2RD, UK
[2] Department of Electrical and Electronics Engineering, Federal University of Technology, PMB 065, Gidan-Kwanu Main Campus, Bida Road, Minna, Niger State, Nigeria
*Corresponding Author: Habibu.Hussaini@nottingham.ac.uk

***Abstract*—Most of the existing methods used to estimate the cable resistance require the use of many hardware devices and the injection of perturbations to the system. Therefore, they are time-consuming, costly and prone to errors. In addition, the injection of perturbations has the potential of degrading the power quality of the system. In this paper, a new artificial neural network (ANN) aided cable resistance estimation approach is proposed. The ANN model is trained by simulation data. The trained ANN model can quickly and effectively map the current sharing ratios between the converters to the droop coefficients of the converters. In this way, the optimal droop coefficient combination that will yield the desired accurate current sharing ratio between the converters can be predicted by the trained ANN model. Subsequently, the optimal droop coefficient combination can be used in the estimation of the corresponding subsystem cable resistance by solving an equation set. The estimated cable resistance is compared with the simulated cable resistance and an excellent match is observed.**

***Keywords—Cable resistance estimation, Neural Network model, converters, droop coefficient, droop control, output DC current***

## I. INTRODUCTION

The more electric aircraft (MEA) electrical power system (EPS) distribution network can be regarded as a typical DC microgrid (MG) architecture, that is made up of multiple sources and operating in the islanding mode [1, 2, 3]. The need to share the load power demand properly among the sources cannot be overemphasised since it will impact the EPS performance, for example, the sources may be overloaded and thermally stressed. Moreover, accurate sharing of load power demand is one of the main control objectives in the low voltage DC MG [4]. This can be realized by the droop control method. However, the conventional droop control method has a limitation in realizing accurate load sharing and voltage regulation due to the influence of unequal cable resistance and nominal voltage reference offset. The unequal cable impedance which is usually a common feature of a low voltage distribution system can be attributed to the difference in the relative distance (geographic location) between the sources and the load in the microgrid [5].

Generally, when high droop coefficients are set for the converters in MG, accurate load sharing among the sources can be guaranteed because the influence of the cable resistance on load sharing becomes negligible. However, this can result in poor regulation of the DC bus voltage, particularly under heavy load conditions (due to high voltage drop). Conversely, when the droop coefficient set for the converters are small, the regulation of the DC bus voltage is enhanced while the load sharing accuracy is degraded [5]. Hence, a trade-off exists between load sharing accuracy and voltage regulation [6]. Therefore, the design of the droop coefficient is very important to achieve a balance between accurate load sharing and voltage regulation. Despite the tradeoff, droop control is still a competitive solution for both small and large distributed DC EPS due to its independence of communication channel, increase in system reliability and modularity.

The line impedance in the low voltage DC microgrid is predominantly resistive [7]. Line impedance information can be used as a basis for many power system analyses such as stability analysis. Also, the information obtained can be used for the control of both grid-connected and islanded EPS, such as the control of power converters and active filters [8, 9], non-linear current controllers, techniques for the detection of the on/off-grid mode of operation [10, 11]. There are various techniques used for the estimation of the line impedance as can be found in [11, 12, 13]. These techniques are classified majorly as passive and active methods. A detailed analysis of the strengths and drawbacks of these methods can be found in [10]. However, most of the methods require the use of many resources which will increase the cost of the system. Furthermore, they are based on the injection of disturbances (such as harmonics) to the system. This will affect the power quality of the system [14, 15]. A quasi-passive technique based on parametric identification is proposed in [10] for the estimation of the line impedance of the electricity distribution network. It was proposed to harness the strengths of the passive and active methods. However, it is also based on the injection of perturbations to the system.

Due to the recent developments in machine learning (ML) and artificial intelligence (AI) based research, there has been an increasing interest in their application for the estimation of electrical power system parameters [16]. The artificial neural network (ANN) method is the most actively researched area for AI application for power electronics systems due to the flexibility of its structure to integrate other AI techniques for performance improvement. Furthermore, the remarkable development in computer hardware provides room for the neural network (NN) to handle complex tasks related to power electronic systems in a seamless manner [17, 18]. A detailed review of machine learning-based approaches such as recurrent neural networks (RNNs), FFNNs, and support vector machine (SVM) in the estimation of battery state is provided in [16].

A NN based approach for the prediction of the insulation resistance of an electrical machine is proposed in [19] to evaluate the machine thermal lifetime. A comparison for the estimation of the lifetime of wire insulation that is subjected to thermal stress using curve-fitting models, neural network and conventional methods is carried out in [20]. An enhanced droop control strategy is proposed in [5, 21], that can ensure accurate current sharing and the restoration of the DC bus voltage to its rated value. This control method compensates for the droop coefficient of each converter according to the estimated corresponding subsystems cable resistances. The line impedance information is obtained using an active identification method in [21], while many hardware devices are required in the measurement of the line resistance in [5]. Hence, this enhanced droop control strategy will increase the cost of the system.

Therefore, in this paper, a NN-aided cable resistance estimation is proposed, neglecting the cable inductance and capacitance. In the first instance, a NN model that requires no knowledge of the corresponding subsystem cable resistance will be employed to determine the optimal droop coefficient of the converters that will yield the desired accurate current sharing ratio between the converters. The proposed approach exploited the excellent generalization capability of the NN to establish a functional relationship between the current sharing ratios between the converters and the droop coefficients of the converters. After data collection from multiple simulations, a NN model can be obtained through offline training. The trained NN model can quickly and effectively map the current sharing ratio between the converters to the droop coefficients of the converters. This way can generate the optimal droop coefficient combination without the need of knowing the corresponding subsystems cable resistance. Subsequently, the optimal droop coefficient combination can then be used in the estimation of the corresponding subsystems cable resistances, just in a few steps. The estimated cable resistance can therefore be used for further power system analysis.

The proposed method makes use of the NN regression model and its excellent nonlinear mapping capabilities between the input and output training data. The process of data collection used for training the NN can be automated. Thus, data collection can be carried out on a multi-core standard computer without monitoring. The data collection process is only required to be carried out once. Moreover, it takes only a few seconds for the NN training after processing the raw data.

## II. Case Study System Description and Analysis of the Conventional Droop Control Method

In this section, a detailed description of the MEA EPS used as a case study and analysis of the conventional droop control method will be provided.

### A. System Description

A generalised parallel-connected multi-source DC grid for the future MEA EPS architecture is shown in Fig. 1. The generators ($G_1$-$G_n$) are assumed to be PMSGs. The main DC bus (270 V) is supplied power by the parallel-connected variable frequency generators. Pulse-width modulated Active front-end controlled rectifier units ($AR_1$-$AR_n$) are employed to control and regulate the output voltage of the corresponding variable frequency generators. The local converter output capacitors are represented as $C_1$-$C_n$ and the main DC bus capacitor bank is $C_b$. The load is a constant power load (CPL).

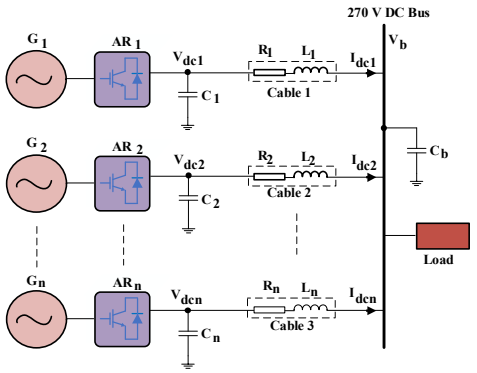


Fig. 1: Multi-source DC grid Architecture for Future MEA EPS

### B. System Control Model

Fig. 2 shows the detailed MEA EPS control model. The two-level voltage source converter (VSC) in Fig. 2 is controlled using the voltage-mode droop control scheme for current sharing among the converters in the MEA EPS. The VSC is an active front end rectifier unit (AR) as shown in Fig. 1. The detailed MEA EPS system model will serve as the basis of the proposed NN-aided cable resistance estimation.

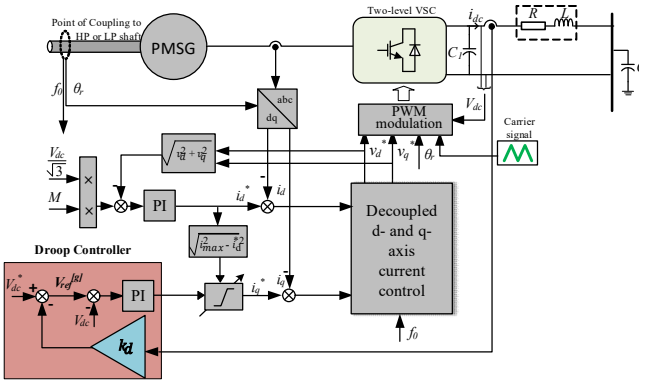


Fig. 2. Voltage-mode Droop Control Scheme of a PMSG fed by an Active Rectifier (AR) in the MEA EPS

### C. Analysis of the Conventional Droop Control Method

In the voltage-mode droop control scheme, the measured branch output DC current is used to generate the reference voltage, and this is expressed in (1).

$$V_{dci}{}^{*} = V_{dc}^{*} - k_{di} I_{dci} \tag{1}$$

where $i$ represent the number of subsystems ($i$ =1,2,3 in this paper since we are considering only three sources), the nominal DC bus voltage (270 V) is $V_{dc}{}^{*}$, the calculated reference voltage for each subsystem converter is denoted as $V_{dci}{}^{*}$, the output current of each converter is $I_{dci}$, the droop coefficient is denoted as $k_{di}$. The current sharing ratio among the sources in steady-state is as expressed in (2), provided the effect of cable impedance on load sharing is negligible.

$$I_{dc1} : I_{dc2} : I_{dc} = \frac{1}{k_{d1}} : \frac{1}{k_{d2}} : \frac{1}{k_{d3}} \tag{2}$$

where each of the converter's droop coefficients is $k_{d1}$, $k_{d2}$ and $k_{d3}$ respectively. The droop coefficient is usually chosen to be proportional to the generators ratings to ensure an accurate current sharing, based on the assumption that the same nominal voltage $V_{dc}{}^{*}$ is applied to each of the droop characteristics.

The cable resistance is unavoidable in a practical situation. When the voltage drop on the cable (in Fig. 2) is considered and the voltage control dynamics are neglected, the steady-state DC bus voltage can be expressed as in (3).

$$V_b = V_{dc}^* - I_{dci}R_i = V_{dc}^* - I_{dci}(k_{di} + R_i) \quad (3)$$

where $V_b$ is the main DC bus voltage, $R_i$ is the resistance of the individual cable connecting the $i$th source to the load. Hence, the current sharing among the sources, assuming they are supplying together can be expressed as

$$I_{dc1}: I_{dc2}: I_{dc3} = \frac{1}{k_{d1}+R_1} : \frac{1}{k_{d2}+R_2} : \frac{1}{k_{d3}+R_3} \quad (4)$$

It can be deduced from (4) that the cable resistance and droop coefficient will have an impact on the current sharing ratio of the sources in steady-states. Also, the branch current of each subsystem is determined by the ratio of the individual droop coefficient.

There are two approaches usually used to mitigate the influence of cable resistance on accurate load sharing. The first approach is to set the droop gain far greater than the cable resistance ($k_{di} \gg R_i$), such that the effect of the cable resistance on load sharing becomes negligible. However, this can only be achieved in a small microgrid where the influence of the cable resistance can be ignored. In a low-voltage DC microgrid such as the MEA EPS, the cable impedance cannot be ignored [5, 22]. The second approach is to compensate for the influence of the cable resistance on accurate current sharing through the modification of the droop coefficient for each of the subsystems according to the corresponding estimated cable resistance as proposed in [5, 14]. The effectiveness of this approach depends solely on the knowledge (accurate measurement) of the corresponding subsystems cable resistance.

Therefore, in this paper, an intelligent approach (i.e. ANN), that requires no knowledge of the corresponding subsystem cable resistance, will be employed in the design of the converters droop coefficients for accurate current sharing.

## III. Proposed NN-aided Cable Resistance Estimation

### A. Mathematical analysis of the proposed approach

From (4), the output DC current sharing ratio between the converters can be calculated based on the expressions in (5) and (6). The output current of converter 1 is used as the base value.

$$n_1 = \frac{I_{dc}}{I_{dc1}} = \frac{k_{d1}+R_1}{k_{d2}+R_2} \quad (5)$$

$$n_2 = \frac{I_{dc3}}{I_{dc1}} = \frac{k_{d1}+R_1}{k_{d3}+R_3} \quad (6)$$

where $n_1$ and $n_2$ are the current sharing ratio between converter 1 and 2, and converter 1 and 3 respectively; $k_{d1}$, $k_{d2}$ and $k_{d3}$ are the conventional droop coefficients for each of converters respectively; $I_{dc1}$, $I_{dc2}$ and $I_{dc3}$ are the inaccurate output DC current of the converters based on the conventional droop coefficients respectively.

It can be observed from (5) and (6) that the current sharing ratios $n_1$ and $n_2$ can be calculated based on the measurement of the output DC currents of the converters. These current sharing ratios will not be as desired due to the influence of the unequal cable resistance on the current sharing performance of the conventional droop control method.

Assuming, a trained NN model can be used to design and predict the optimal droop coefficients of the converter to yield accurate current sharing in the desired sharing ratio. Hence, we can obtain the expression in (7) and (8).

$$n_{1desire} = \frac{I_{dc2ne}}{I_{dc1new}} = \frac{k_{d1o}+R_1}{k_{d2op}+R_2} \quad (7)$$

$$n_{2desired} = \frac{I_{dc3ne}}{I_{dc1new}} = \frac{k_{d1op}+R_1}{k_{d3opt}+R_3} \quad (8)$$

where $n_{1desired}$ and $n_{2desired}$ are the desired accurate current sharing ratio between converter 1 and 2, and converter 1 and 3 respectively; $k_{d1opt}$, $k_{d2opt}$ and $k_{d3opt}$ are the NN model-predicted optimal droop coefficients for each of converters respectively; $I_{dc1new}$, $I_{dc2new}$ and $I_{dc3new}$ are the accurate output DC current of the converters based on the optimal droop coefficients respectively. Therefore, for a desired accurate and equal current sharing ratio between the converters, the expression in (7) and (8) can be re-written as

$$n_{1desired} = 1 = \frac{k_{d1opt}+R_1}{k_{d2opt}+R_2} \quad (9)$$

$$n_{2desired} = 1 = \frac{k_{d1opt}+R_1}{k_{d3opt}+R_3} \quad (10)$$

By solving the equation from (5) to (10), the expressions for $R_1$, $R_2$ and $R_3$ can be obtained as follows:

$$R_1 = \frac{\left(\frac{k_{d1}}{n_1} - k_{d2} + k_{d2opt} - k_{d1opt}\right)}{\left(1 - \frac{1}{n_1}\right)} \quad (11)$$

$$R_2 = \frac{k_{d1}+R_1}{n_1} - k_{d2} \quad (12)$$

$$R_3 = \frac{k_{d1}+R_1}{n_2} - k_{d3} \quad (13)$$

Therefore, the corresponding subsystems cable resistances $R_1$, $R_2$ and $R_3$ can be estimated from (11), (12) and (13) respectively, by knowing the conventional design point (from (5) and (6)) and the final optimal design point from NN-based method.

### B. NN-based Optimal Droop Coefficient Design

By sweeping the combinations of the droop coefficients in the design space, the training data can be collected from a series of simulations. Then, the desired NN can be trained efficiently. The trained NN can be used to predict the optimal droop coefficients combination that will yield the desired accurate current sharing. Thereafter, the predicted optimal droop coefficient combination can then be used in the estimation of the corresponding subsystems cable resistances.

A flow chart showing the design steps to be followed in the NN-based optimal droop coefficient design approach is shown in Fig. 3.

There are three stages involved in the design of the optimal droop coefficients of the converters to yield the desired accurate current sharing ratio as highlighted in Fig. 3. In the first stage, data is collected from a detailed simulation of the MEA EPS model shown in Fig. 2. For every combination of

the droop coefficients ($k_{d1}$, $k_{d2}$, and $k_{d3}$) within the design space, the corresponding inaccurate output DC currents of the converters ($I_{dc1}$, $I_{dc2}$, and $I_{dc3}$) are obtained. Thereafter, the current sharing ratio between the converters is computed ($n_1 = I_{dc2}/I_{dc1}$ and $n_2 = I_{dc3}/I_{dc1}$). At this stage, the droop coefficients combinations serve as input to the simulation model. The sweep range of the droop coefficient should be pre-defined in such a manner that it covers a feasible design space for the desired sharing ratio.

In the second stage, the data generated is used to train the NN. Before training the NN model, the current sharing ratios between the converters (i.e. $n_1$ and $n_2$) are first determined for all the output DC currents of the converters ($I_{dc1}$, $I_{dc2}$, and $I_{dc3}$) within the design space. The NN model will be trained with $n_1$ and $n_2$ as input and the droop coefficient combinations (i.e. $k_{d1}$, $k_{d2}$ and $k_{d3}$) as the targeted output. Thereafter, the trained NN becomes a dedicated surrogate model of the converter.

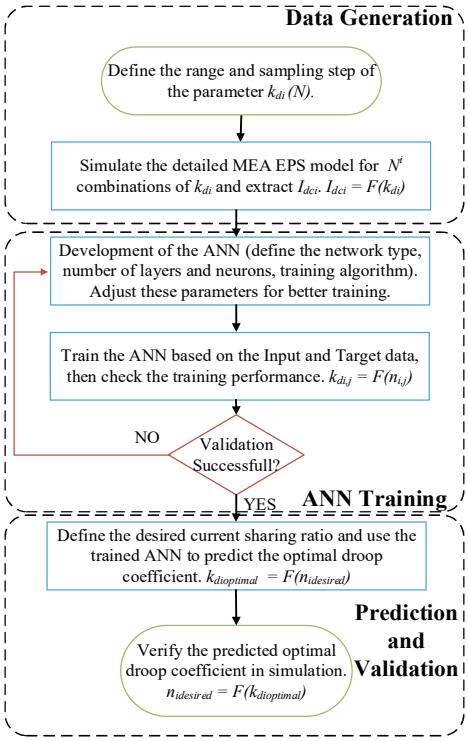

Fig. 3: Flowchart for the design of the Droop Coefficient using the ANN approach

In the third stage, based on a user-defined desired current sharing ratio, the optimal droop coefficient combination that will yield the desired current sharing ratio can be predicted by the trained NN in a fast and accurate manner. The surrogate model can generate results in several orders of magnitude faster when compared to the detailed simulation model which is a big gain. It is noteworthy to mention that the data generation and training of the NN steps need to be carried out only once for a particular detailed system model and parameters [23].

*1) Data generation*

The detailed MEA EPS system control model shown in Fig. 3 was developed using the MATLAB SIMULINK©. A CPL of 40 kW was applied to the MEA EPS at 0.04 s during data generation. The MEA EPS and its equivalent DC cable parameters used in the simulation are as shown in TABLE I and II respectively.

TABLE I. ELECTRICAL POWER SYSTEM PARAMETERS

| Parameter | Symbol | Value |
|---|---|---|
| Rated Voltage of main DC Bus | $V_{dc}^*$ | 270 V |
| Local Shunt Capacitor | $C_i$ | 1.2 mF |
| Main DC bus capacitor | $C_b$ | 0.6 mF |
| Converter 1 Droop gain | $k_{d1}$ | 1/4.250 |
| Converter 2 Droop gain | $k_{d2}$ | 1/4.250 |
| Converter 3 Droop gain | $k_{d3}$ | 1/4.250 |

TABLE II. EQUIVALENT DC CABLES PARAMETERS

| | Resistance ($R_i$)-(0.6 mΩ/m) | Inductance ($L_i$) -(0.2 µH /m) | Length (m) |
|---|---|---|---|
| Cable 1 | 3 mΩ | 1 µH | 5 |
| Cable 2 | 30 mΩ | 10 µH | 50 |
| Cable 3 | 15 mΩ | 5 µH | 25 |

For the NN-based optimal droop coefficient design, the sweep range (i.e. design space) is selected based on the conventional droop coefficient settings of the converters shown in TABLE I for the desired equal current sharing ratio between the converters. Furthermore, the droop coefficient sweep range is selected to cover $\pm$10% of the conventional droop coefficients to ensure a feasible design space with high fidelity as shown in TABLE III. The sweep range and sampling step of the droop coefficients ($k_{d1}$, $k_{d2}$, $k_{d3}$) used in the simulation for data generation are as presented in TABLE III.

TABLE III. DESIGN OF THE SWEEP VALUES

| Variable | Range | Sampling Step | No. of Samples |
|---|---|---|---|
| $k_{d1}$ | [1/3.825 1/4.675] | 0.085 | 11 x 11 x 11 = 1331 |
| $k_{d2}$ | [1/3.825 1/4.675] | 0.085 | |
| $k_{d3}$ | [1/3.825 1/4.675] | 0.085 | |

It can be observed from TABLE III that 11 settings for each of the droop coefficients were tested, thereby making a total of $N^i = 11^3 = 1331$ combinations of the droop coefficient. Multiple simulations are carried out for every combination of the droop coefficients ($k_{d1}$, $k_{d2}$, $k_{d3}$) and the output DC current ($I_{dc1}$, $I_{dc2}$, $I_{dc3}$) of the converters are obtained and recorded from each of the simulations. This makes a total of 1331x6 data generated for training the NN.

The multiple simulations were carried out in a loop and the process was automated with the aid of MATLAB codes developed and run from a MATLAB script file. The simulation process can be fast-tracked on a standard multi-core computer using the parallel computing tool in MATLAB [24]. In this paper, the simulations were carried out on a standard personal computer with a quad-core processor. The data generated from the multiple simulations were obtained within around 4 hours.

*2) Structure and Training of the NN*

In this paper, the FFNN structure is selected to train the NN due to the static relationship between the input and output data [23]. A typical FFNN structure comprises an input layer, one or more hidden layers and an output layer. A very important factor in the training of the neural network is the number of hidden layer neurons. The neurons present in each layer process the information emanating from the neurons in the preceding layer. A detailed description of the FFNN can be found in [18].

The structure of the proposed NN model is shown in Fig. 4. It consists of an input layer with 2 neurons, a hidden layer with 11 neurons and an output layer with 3 neurons. The 2

neurons in the input layer correspond to the calculated output DC current sharing ratio between the converters ($n_1$, and $n_2$), while the 3 neurons in the output layer represent the droop coefficients ($k_{d1}$, $k_{d2}$ and $k_{d3}$). After training, the NN model can be used to predict the optimal droop coefficient combination with a user-defined desired current sharing ratio input. The training was implemented in MATLAB's Neural Network Toolbox. A detailed description of the NN structure and training process can be found in [17, 18, 25].

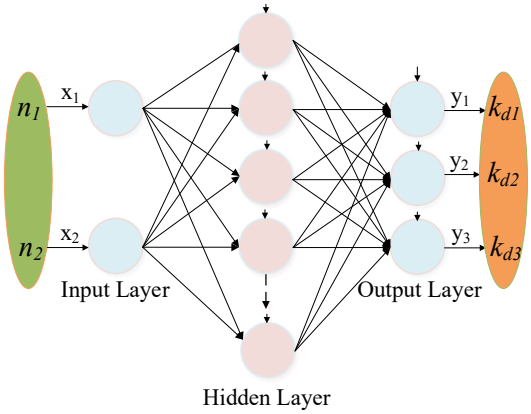


Fig. 4: Structure of the three-layer FFNN which serves as a surrogate model of the MEA EPS model shown in Fig. 3. The internal weights and bias terms are not included for simplicity.

It was observed that in developing the structure of the NN model and before training, that the choice of the number of neurons used in the hidden layer(s) to train the NN has a significant impact on the model's performance (overfitting or underfitting). A general rule is to start with a relatively small number of neurons and then increase it gradually based on the observed training error [17]. This is a trial-and-error process and can be carried out very fast since the training can be completed within a few seconds [24]. In this paper and for the MEA EPS studied, the 11 neurons selected in the hidden layer of the NN structure used for training provides a very good match between the training data obtained from the detailed simulation model and the NN model prediction as shown in Fig. 5.

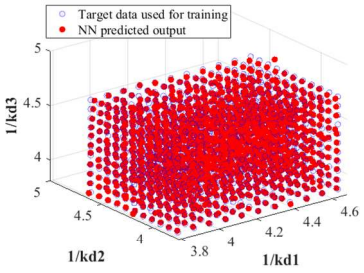


Fig. 5. Comparison between the droop coefficient combinations used as input to the detailed MEA EPS model and the NN model prediction

The root mean squared error (RMSE) is used to validate the performance of the NN model training in this paper. The RMSE is the absolute difference between the predicted output of the trained NN model (inputs are $n_1$ and $n_2$ in training data) and the targeted coefficient data used in training. The closer the RMSE value to zero, the better the training performance of the NN (its predictive capability). TABLE IV shows the calculated RMSE, hence, the NN is well trained.

TABLE IV. NN PREDICTION ERROR OF THE TRAINING DATA

| Parameters | $k_{d1}$ | $k_{d2}$ | $k_{d3}$ |
|---|---|---|---|
| RMSE | 0.031939 | 0.031005 | 0.033269 |

*3) Deployment of the Trained NN model for Prediction*

After training, the NN model has now established a functional relationship between the inaccurate output DC current sharing ratio between the converters due to the influence of the unequal cable resistance and the droop coefficient combinations. The user can now define the desired output DC current sharing ratio between the converters (i.e. $n_{1desired}$ and $n_{2desired}$) and the trained NN model is expected to predict the droop coefficient combination that will yield the $n_{1desired}$ and $n_{2desired}$.

In this paper and for the three sources MEA EPS studied, $n_{1desired}$ and $n_{2desired}$ are both set as 1 for the equal current sharing of the load current demand. The predicted droop coefficient combination by the trained NN model for the desired sharing ratio is as shown in TABLE V.

TABLE V. NN PREDICTED OPRIMAL DROOP COEFFICIENTS

| Desired ratio | *Predicted Optimal droop coefficients* | | |
|---|---|---|---|
| $n_{1desired} = 1$ | $k_{d1}^{pred}$ | $k_{d2}^{pred}$ | $k_{d3}^{pred}$ |
| $n_{2desired} = 1$ | 1/3.9850 | 1/4.4650 | 1/4.1850 |

A graphical plot of the desired current sharing ratio and the predicted optimal droop coefficient combination is as shown in Fig. 6 (a) and (b) respectively

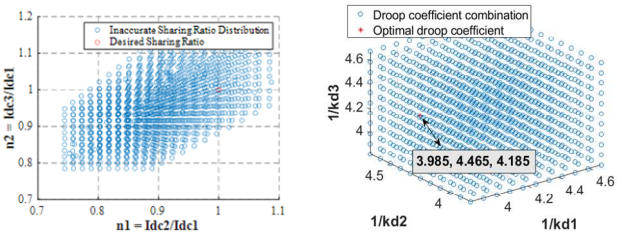


Fig. 6. (a) Plot of the distribution of the calculated output DC current sharing ratio used as input to the trained NN Model. The user-defined desired current sharing ratio ($n_{1desired} = 1$ and $n_{2desired} = 1$) is indicated with a Red cycle. (b) A plot of the distribution of the 1331 droop coefficient combinations which serve as the target output used to train the NN model. The optimal droop coefficients combination predicted by the trained NN model that will yield the desired accurate output DC current sharing ratio is indicated with a Red cycle.

## IV. VALIDATION OF THE PROPOSED NN-AIDED CABLE RESISTANCE ESTIMATION

A simulation study was carried out to validate that the optimal droop coefficient combination predicted by the trained NN model will yield the desired current sharing ratio as shown in TABLE V. Furthermore, a comparison of the performance of the conventional droop control using the conventional droop coefficient shown in TABLE I and the predicted optimal droop coefficient was conducted. The simulation parameters used for the validation and comparison are the same as shown in TABLE I and TABLE II. A CPL of 40 kW was applied at 0.04 s during the simulation. A summary of the simulation results is shown in TABLE VI.

TABLE VI. SUMMARY OF THE SIMULATION RESULT OF THE VALIDATION OF THE PREDICTED OPTIMAL DROOP COEFFICIENT AND BY THE TRAINED NN MODEL

| $k_{d1opt}$ | $k_{d2opt}$ | $k_{d3opt}$ | $I_{dc1new}$ (A) | $I_{dc2new}$ (A) | $I_{dc3new}$ (A) |
|---|---|---|---|---|---|
| 1/3.985 | 1/4.465 | 1/4.185 | 51.920 | 51.920 | 51.920 |
| $k_{d1}$ | $k_{d2}$ | $k_{d3}$ | $I_{dc1}$ (A) | $I_{dc2}$ (A) | $I_{dc3}$ (A) |
| 1/4.250 | 1/4.250 | 1/4.250 | 54.610 | 49.056 | 51.990 |

It can be observed from TABLE VI that the predicted optimal droop coefficient by the trained NN model can yield the desired current sharing ratio between the converters ($n_{1desired}$ = 1 and $n_{2desired}$ =1). Hence, the optimal droop coefficient combination can mitigate the influence of the corresponding subsystems cable resistances on accurate current sharing. Conversely, the current sharing ratios between the converters in steady-state using the conventional droop coefficients are $n_1$ = 0.8983 and $n_2$ = 0.9520. The graphical simulation results of the comparison are as shown in Fig. 7 (a) and (b) using the conventional droop coefficients and the optimal droop coefficient respectively.

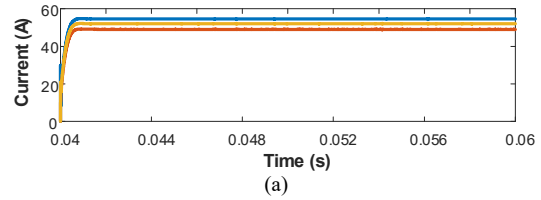


(a)

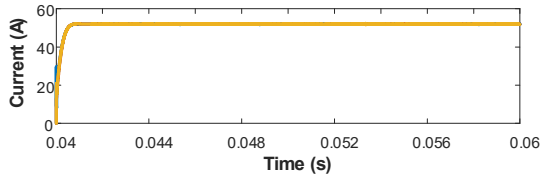


(b)

Fig. 7. Comparison of the simulation results of the current sharing performance of the conventional droop control method for desired current sharing ratio (1:1) (a) Using the conventional droop coefficient (b) Using the optimal droop coefficient predicted by the trained NN model

After the validation of the predicted optimal droop coefficient, the values of $n_1$, $n_2$, $k_{d1opt}$, $k_{d2opt}$ and $k_{d3opt}$ can now be substituted into (11), (12) and (13) to estimate the corresponding subsystems cable resistances $R_1$, $R_2$ and $R_3$ respectively. The result of the substitutions is as shown in TABLE VII.

TABLE VII. RESULT OF THE VALIDATION OF THE PROPOSED NN-AIDED CABLE RESISTANCE ESTIMATION

| Simulated $R_i$ (mΩ) | Estimated $R_i$ (mΩ) | Error (%) |
|---|---|---|
| 3 | 2.988 | 0.4 |
| 30 | 29.97 | 0.1 |
| 15 | 14.95 | 0.3 |

It can be observed from TABLE VII that the simulated and estimated cable resistance matched excellently well.

## V. CONCLUSION

The neural network approach is employed to develop a tool for the fast and accurate estimation of cable resistance in a droop-controlled islanded DC microgrid. The proposed approach can realize the desired current sharing performance of the conventional droop control method based on the predicted optimal droop coefficient combination by the trained NN model. The predicted optimal droop coefficient combination can then in turn be used for the estimation of the corresponding subsystems cable resistances. There is an excellent match between the estimated cable resistance and the simulated cable resistance. The estimated cable resistance can therefore be used for the desired power system analysis and control operations.

## ACKNOWLEDGMENT

This work has received funding from the Clean Sky 2 Joint Undertaking under the European Union's Horizon 2020 research and innovation programme under grant agreement No 807081. The author Habibu Hussaini extends his profound appreciation to the Petroleum Technology Development Fund (PTDF), Nigeria, for the scholarship funding.

## REFERENCES

[1] A. Barzkar and M. Ghassemi, "Electric power systems in more and all electric aircraft: A Review," *IEEE Access*, pp. 169314 - 169332, 2020.

[2] H. Hussaini, T. Yang, C. Wang and S. Bozhko, "An Enhanced and Cost Saving Droop Control Method for Improved Load Sharing for the MEA Application," in *2021 IEEE Transportation Electrification Conference & Expo (ITEC)*, pp. 84-89, Chicago, IL, USA, 2021.

[3] Z. Huang, T. Yang, P. Giangrande, M. Galea and P. Wheeler, "Technical Review of Dual Inverter Topologies for More Electric Aircraft Applications," *IEEE Transactions on Transportation Electrification*, 2021.

[4] S. Anand and B. G. Fernandes, "Steady state performance analysis for load sharing in DC distributed generation system," in *2011 10th International Conference on Environment and Electrical Engineering*, pp. 1-4, 2011.

[5] A. Tah and D. Das, " An enhanced droop control method for accurate load sharing and voltage improvement of isolated and interconnected DC microgrids," *IEEE Transactions on Sustainable Energy*, vol. 7, no. 3, pp. 1194-1204, 2016.

[6] J. M. Guerrero, M. Chandorkar, T. L. Lee and P. C. Loh, "Advanced control architectures for intelligent microgrids—Part I: Decentralized and hierarchical control," *IEEE Transactions on Industrial Electronics*, vol. 60, no. 4, pp. 1254-1262, April 2013.

[7] Z. Shuai, D. He, J. Fang, Z. J. Shen, C. Tu and J. Wang, "Robust droop control of DC distribution networks," *IET Renewable Power Generation*, vol. 10, no. 6, pp. 807-814, 2016.

[8] A. Tarkiainen, R. Pollanen, M. Niemela and J. Pyrhonen, "Identification of grid impedance for purposes of voltage feedback active filtering," *IEEE Power Electronics Letters*, vol. 2, no. 1, pp. 6-10, 2004.

[9] M. Sumner, A. Abusorrah, D. Thomas and P. Zanchetta, "Improved power quality control and intelligent protection for grid connected power electronic converters, using real time parameter estimation," in *2006 IEEE Industry Applications Conference Forty-First IAS Annual Meeting*, Vol. 4, pp. 1709-1715, Tampa, USA, 2006, October.

[10] M. Ciobotaru, V. Agelidis and R. Teodorescu, "Line impedance estimation using model based identification technique," in *2011 14th European Conference on Power Electronics and Applications*, pp. 1-9, Birmingham, UK, 2011, August.

[11] A. V. Timbus, R. Teodorescu and P. Rodriguez, "Grid impedance identification based on active power variations and grid voltage control," in *2007 IEEE Industry Applications Annual Meeting*, pp. 949-954, New Orleans, USA, 2007, September.

[12] M. Sumner, B. Palethorpe, D. W. Thomas, P. Zanchetta and M. C. Di Piazza, " A technique for power supply harmonic impedance estimation using a controlled voltage disturbance," *IEEE Transactions on Power Electronics*, vol. 17, no. 2, pp. 207-215, 2002.

[13] L. Asiminoaei, R. Teodorescu, F. Blaabjerg and U. Borup, "Implementation and test of an online embedded grid impedance estimation technique for PV inverters," *IEEE Transactions on Industrial Electronics*, vol. 52, no. 4, pp. 1136-1144, 2005.

[14] C. Liu, J. Zhao, S. Wang, W. Lu and K. Qu, "Active identification method for line resistance in DC microgrid based on single pulse injection," *IEEE Transactions on Power Electronics*, vol. 33, no. 7, pp. 5561-5564, July 2018.

[15] H. Gu, X. Guo, D. Wang and W. Wu, "Real-time grid impedance estimation technique for grid-connected power converters," in *2012 IEEE International Symposium on Industrial Electronics*, Hangzhou, China, May 2012.

[16] C. Vidal, P. Malysz, P. Kollmeyer and A. Emadi, "Machine learning applied to electrified vehicle battery state of charge and state of health estimation: State-of-the-art," *IEEE Access*, vol. 8, pp. 52796-52814, 2020.

[17] S. Zhao, F. Blaabjerg and H. Wang, "An overview of artificial intelligence applications for power electronics," *IEEE Transactions on Power Electronics*, vol. 36, no. 4, pp. 4633 - 4658, 2021.

[18] B. K. Bose, "Neural network applications in power electronics and motor drives—An introduction and perspective," *IEEE Transactions on Industrial Electronics*, vol. 54, no. 1, pp. 14-33, 2007.

[19] G. Turabee, M. R. Khowja, V. Madonna, P. Giangrande, G. Vakil, C. Gerada and M. Galea, "Thermal Lifetime Evaluation of Electrical Machines Using Neural Network," in *2020 IEEE Transportation Electrification Conference & Expo (ITEC)*, pp. 1153-1158, Chicago, USA, 2020, June.

[20] M. R. Khowja, G. Turabee, P. Giangrande, V. Madonna, G. Cosma, G. Vakil, C. Gerada and M. Galea, "Lifetime estimation of enameled wires under accelerated thermal aging using curve fitting methods," *IEEE Access*, vol. 9, pp. 18993-19003, 2021.

[21] W. Jiang, J. Zhao, K. Qu, L. Mao, Y. Zhu and H. Liu, "An Enhanced Drop Control Method for DC Microgrids with Accurate Current Sharing and DC Bus Voltage Restoration," in *2019 4th International Conference on Intelligent Green Building and Smart Grid (IGBSG)*, Hubei, China, 2019.

[22] N. Yang, D. Paire, F. Gao, A. Miraoui and W. Liu, "Compensation of droop control using common load condition in DC microgrids to improve voltage regulation and load sharing," *International Journal of Electrical Power & Energy Systems*, vol. 64, pp. 752-760, 2015.

[23] M. Novak, T. Dragicevic and F. & Blaabjerg, "Weighting factor design based on Artificial Neural Network for Finite Set MPC operated 3L-NPC converter," in *2019 IEEE Applied Power Electronics Conference and Exposition (APEC)*, pp. 77-82, Anaheim, CA, USA, March 2019.

[24] T. Dragičević and M. Novak, "Weighting factor design in model predictive control of power electronic converters: An artificial neural network approach," *IEEE Transactions on Industrial Electronics*, vol. 66, no. 11, pp. 8870-8880, Nov. 2019.

[25] Z. Xu, Y. Gao, X. Wang, X. Tao and Q. Xu, "Surrogate thermal model for power electronic modules using artificial neural network," in *IECON 2019-45th Annual Conference of the IEEE Industrial Electronics Society*, pp. 3160-3165, Lisbon, Portugal, 2019.